



# Chemical complexity induced local structural distortion in NiCoFeMnCr high-entropy alloy

Fuxiang Zhang, Yang Tong, Ke Jin, Hongbin Bei, William J. Weber, Ashfia Huq, Antonio Lanzirotti, Matt Newville, Darren C. Pagan, J. Y. P. Ko & Yanwen Zhang

To cite this article: Fuxiang Zhang, Yang Tong, Ke Jin, Hongbin Bei, William J. Weber, Ashfia Huq, Antonio Lanzirotti, Matt Newville, Darren C. Pagan, J. Y. P. Ko & Yanwen Zhang (2018) Chemical complexity induced local structural distortion in NiCoFeMnCr high-entropy alloy, Materials Research Letters, 6:8, 450-455, DOI: [10.1080/21663831.2018.1478332](https://doi.org/10.1080/21663831.2018.1478332)

To link to this article: <https://doi.org/10.1080/21663831.2018.1478332>



© 2018 Oak Ridge National Laboratory.  
Published by Informa UK Limited, trading as  
Taylor & Francis Group



Published online: 16 Jun 2018.



Submit your article to this journal [↗](#)



Article views: 2319



View related articles [↗](#)



View Crossmark data [↗](#)



Citing articles: 25 View citing articles [↗](#)



ORIGINAL REPORT



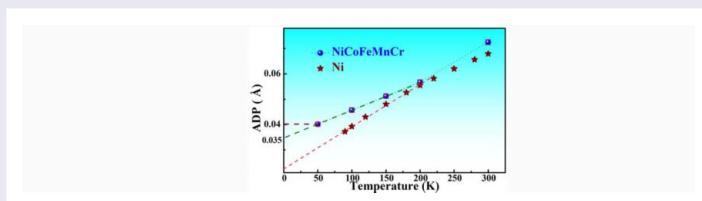
## Chemical complexity induced local structural distortion in NiCoFeMnCr high-entropy alloy

Fuxiang Zhang <sup>a</sup>, Yang Tong <sup>a</sup>, Ke Jin<sup>a</sup>, Hongbin Bei <sup>a</sup>, William J. Weber <sup>a,b</sup>, Ashfia Huq<sup>c</sup>, Antonio Lanzirotti<sup>d</sup>, Matt Newville<sup>d</sup>, Darren C. Pagan<sup>e</sup>, J. Y. P. Ko<sup>e</sup> and Yanwen Zhang <sup>a</sup>

<sup>a</sup>Division of Materials Science and Technology, Oak Ridge National Laboratory, Oak Ridge, TN, USA; <sup>b</sup>Department of Materials Science and Engineering, The University of Tennessee, Knoxville, TN, USA; <sup>c</sup>Spallation Neutron Source, Oak Ridge National Laboratory, Oak Ridge, TN, USA; <sup>d</sup>University of Chicago, Center for Advanced Radiation Sources, Chicago, IL, USA; <sup>e</sup>Cornell High Energy Synchrotron Source, Cornell University, Ithaca, NY, USA

### ABSTRACT

In order to study chemical complexity-induced lattice distortion in high-entropy alloys, the static Debye–Waller (D-W) factor of NiCoFeMnCr solid solution alloy is measured with low temperature neutron diffraction, ambient X-ray diffraction, and total scattering methods. The static atomic displacement parameter of the multi-element component alloy at 0 K is 0.035–0.041 Å, which is obvious larger than that of element Ni ( $\sim 0$  Å). The atomic pair distance between individual atoms in the alloy investigated with extended X-ray absorption fine structure (EXAFS) measurements indicates that Mn has a slightly larger bond distance ( $\sim 0.4\%$ ) with neighbor atoms than that of others.



### IMPACT STATEMENT

The chemical complexity induced local structural disorder in the high entropy alloy is distinguished from the thermal contribution by the combination of neutron and X-ray techniques.

### ARTICLE HISTORY

Received 5 April 2018

### KEYWORDS

Solid solution alloys; neutron diffraction; EXAFS; local structure

The discovery of multi-element concentrated solid solution alloys or high-entropy alloys stimulate the ideals of design new metal alloys and even ceramics with complex chemical compositions [1–5]. As a new class of materials, the compositionally complex alloys have attracted intense research interests over the past decade, leading to the discovery of some HEAs with excellent properties, such as high strength [6,7], good wear, corrosion and irradiation resistance [8–10]. Though HEAs do not always have high configurational entropy, the high entropy effect is still the signature concept of HEAs, and many of the advanced mechanical properties originate from the ‘cocktail’ effect [3]. Due to the lack of chemical periodicity and different atomic sizes, structural distortion is one of the ‘core effects’ in HEAs, which affects the mechanical and physical properties including enhanced hardness [4,11], reduced electrical and thermal

conductivity [12]. However, severe lattice distortion may also destabilize the single solid solution phase. Recent TEM experiments have revealed that both NiCoFeMnCr and NiCoFeCr precipitate after long-time annealing at intermediate temperatures [13–15]. The study of lattice distortion is very important in understanding the advanced mechanical and physical properties of HEAs. Previous investigations suggest that the degree of structural distortion of HEAs varies depending on the different lattice symmetries and chemical compositions [16–19]. An obvious lattice distortion was observed in the bcc solid solution alloy [16], however, the chemical complexity-induced static displacement of atoms in fcc HEAs may not be as large as hypothesized [20].

As a typical example, the five-element HEA NiCoFeMnCr has been extensively studied, and it exhibits damage tolerance with tensile strength above 1 GPa and fracture

toughness values exceeding  $200 \text{ MPa} \cdot \text{m}^{-1/2}$ , and both strength and ductile improve at cryogenic temperatures [21]. The mechanical strengthening in HEAs is believed to be attributed to dislocation activities [6,22]. By analyzing the width of Bragg diffraction peaks from the neutron total scattering profiles [20], NiCoFeMnCr solid solution alloy does not yield significant difference in lattice distortion from that of binary NiCr solid solution alloys with Cr concentration of 20%, 25% and 33%, respectively. Our quantitative analysis [23] of hard X-ray atomic pair distribution function (PDF) has found that the lattice distortion in NiCoFeMnCr is less than 0.24%. This slight lattice distortion is attributed to the chemical complexity which may play a critical role to the mechanical properties. Total scattering methods at ambient temperature can only give an average estimation of the lattice distortion but cannot distinguish the contribution from thermal vibration and static lattice distortion, and the information of individual atomic pairs is also missing.

Local disorders in HEAs result from static lattice distortion and short-range chemical ordering. Short-range order is not rare in traditional alloys and it greatly affects the physical properties [24], and it is also found in HEAs [25,26]. Recent experimental study [27] has revealed complicated magnetic behaviors for NiCoFeMnCr solid solution alloy, which transfers from paramagnetic to a spin glass state at 93 K and then to a ferromagnetic state at 38 K while maintaining its fcc structure down to 3 K. The transition is likely associated with a ferromagnetic ordering of moments carried by Fe, Co, and/or Mn atoms. In this study, through the combination of different experimental techniques, including room temperature hard X-ray total scattering, low temperature time-of-flight neutron diffraction (ND) and extended X-ray absorption fine structure (EXAFS), the intrinsic lattice distortion from the chemical complexity and the local bonding environment of individual elements in NiCoFeMnCr solid solution alloy are investigated.

Solid solution alloy ingot was prepared by arc-melting of high purity element mixtures for more than five times, and finally casted into a copper mold. The polycrystalline alloy sample was made by cold-rolling of the ingot, which was annealed at high temperature ( $1200^\circ\text{C}$ ) for one day. The cold-rolled specimens were then annealed at  $800^\circ\text{C}$  for 1 h. X-ray diffraction measurement confirmed that NiCoFeMnCr sample is a single solid solution phase with a fcc structure. Scanning electron microscope observation revealed that the grain size of the polycrystalline sample is less than  $10 \mu\text{m}$ . The sample was cut into stripes with thickness around  $150 \mu\text{m}$ , mechanically polished and the damaged surface layer was then removed by electrochemical corrosion. The texture and total X-ray scattering measurement was conducted with a

61.332 keV hard X-ray source at CHESS. The instrument parameters were calibrated with a standard  $\text{CeO}_2$  powder from NIST. In order to reduce the effect of texture on the intensity of Bragg peaks, the alloy stripe was rotated during the measurement with  $\omega$  from  $-60^\circ$  to  $60^\circ$  and the final XRD profile was converted from the stacking Debye images with Fit 2d software [28]. The ND measurement was conducted at POWGEN station, Spallation Neutron Source at Oak Ridge National Laboratory with time-of-flight neutron source from room temperature to 50 K. The quantitative structural analysis of the X-ray and ND profiles was performed by using Rietveld refinement method with the Fullprof software [29]. EXAFS spectrum was collected at beam 13-ID-E, Advanced Photon Source at Argonne National Laboratory. The EXAFS at the K-edge of each element was measured in fluorescence mode. The beam size is  $100 \times 100 \mu\text{m}^2$  and nearly perpendicular to the sample surface. X-ray fluorescence was collected in grazing exit mode with angle of 2–3 degrees. The analysis of Fourier Transforms (FTs) of EXAFS and fitting were conducted using Demeter software [30].

X-ray diffraction measurement has indicated that the cold-rolled NiCoFeMnCr single phase solid solution alloy is slightly textured along  $\langle 200 \rangle$  direction. With  $\omega$  scan from  $-60^\circ$  to  $60^\circ$ , no obvious texture is observed and the XRD profile is well refined with a random solid solution structure model. Figure 1(a) shows the Rietveld refinement results and the lattice constant is  $3.5993(1) \text{ \AA}$ . There is no obvious mismatch for the position of Bragg peaks, which suggests that the lattice distortion from the fcc structure is not visible from the XRD measurement. NiCoFeMnCr has a simple fcc structure like Ni, careful analysis of the diffraction patterns can obtain more structural information. Not taking into account the lattice strain, Rietveld refinement yields the isotropic thermal factor  $B_{\text{iso}} = 0.37(3) \text{ \AA}^2$ . Since a severe lattice distortion in a solid solution alloy generates large diffuse scattering, the peak changes due to atomic displacements can also be measured with the total scattering measurements. Analysis of atomic pair distribution function (PDF) found  $\sim 0.24\%$  lattice distortion [23], which is smaller than the expected value due to atomic size mismatch. If neglecting the difference of the individual atoms, the refined isotropic Debye factor  $U_{\text{iso}} = 0.005 \text{ \AA}^2$ , which is very close to the XRD result ( $0.0047 \text{ \AA}^2$  from  $B_{\text{iso}} = 8\pi^2 U_{\text{iso}}$ ). The Debye factor includes the contribution of thermal vibration and static lattice distortion that cannot be distinguished from a room temperature XRD measurement.

Neutrons interact directly with the nuclei of atoms, and ND is more sensitive to the vibration of atoms in solids. NiCoFeMnCr solid solution alloy was measured with time-of-flight ND from room temperature to 50 K. Figure 1(b) shows the Rietveld refinement of the ND

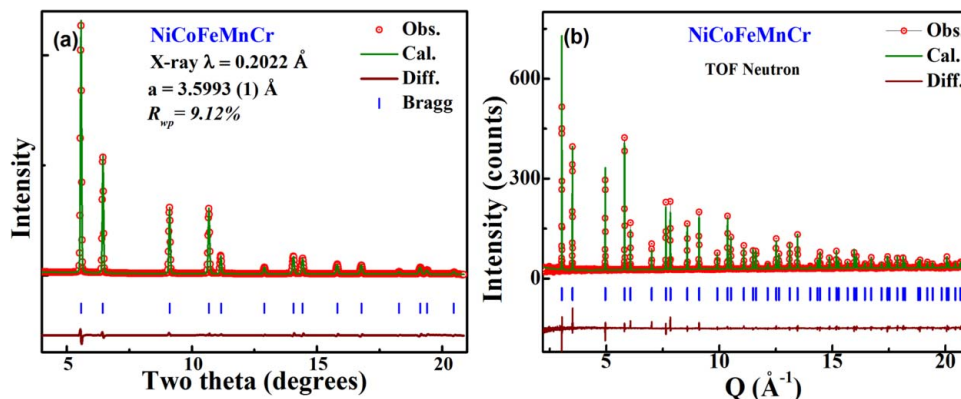


**Figure 1.** Rietveld refinement of NiCoFeMnCr solid solution alloy (a) X-ray diffraction at room temperature (b) time-of-flight ND at 50 K.

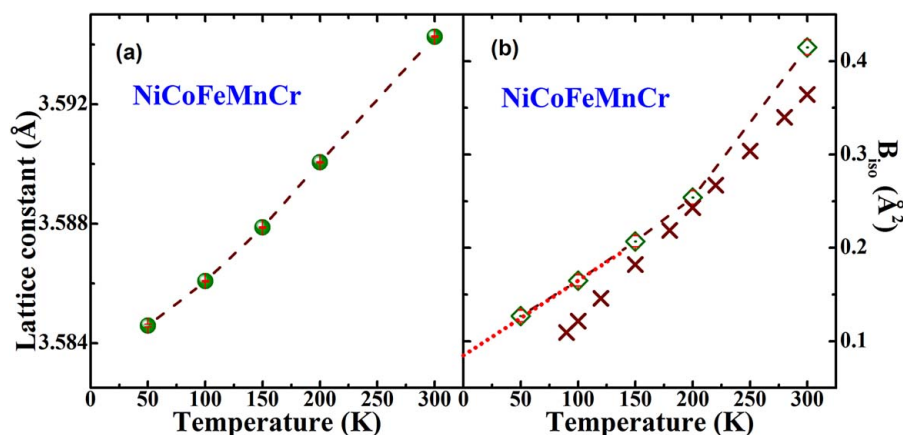


**Figure 2.** Temperature dependence of a) lattice parameter and b) isotropic thermal factors of NiCoFeMnCr solid solution alloy. The cross symbols are the  $B_{180}$  factors of Ni as a comparison.

profile at 50 K. The lattice parameter changes from 3.5942 (1)  $\text{\AA}$  at room temperature to 3.5851 (1)  $\text{\AA}$  at 50 K. Previous low temperature XRD measurements [27] have revealed that the lattice parameter of fcc NiCoFeMnCr alloy reaches the lowest value at 50 K and has no obvious change at lower temperatures though it has a magnetic phase transition at 39 K. At room temperature, the refinement of ND profile yields a thermal factor  $B_{180} = 0.393$  (9)  $\text{\AA}^2$  (or  $U_{180} = 0.005 \text{\AA}^2$ ). The very good agreement of the Debye factors obtained from XRD, X-ray PDF and ND suggested that the Rietveld analysis for our sample is reliable. The temperature dependence of the lattice parameter and Debye factor from ND measurements are illustrated in Figure 2. The Debye factor changes to 0.151 (6)  $\text{\AA}^2$  ( $U_{180} = 0.020 \text{\AA}^2$ ) at 50 K. By linear extrapolating the thermal factor to 0 K,  $B_{180} = 0.09 \text{\AA}^2$  and  $U_{180} = 0.001 \text{\AA}^2$  are obtained. The thermal vibration is close to zero to most materials as shown in Figure 2(b) for Ni [31]. Assuming the thermal vibration for NiCoFeMnCr at 0 K is zero, the Debye factor of 0.001  $\text{\AA}^2$  at 0 K is the intrinsic vibration which can only be contributed by the size mismatch of different elements,

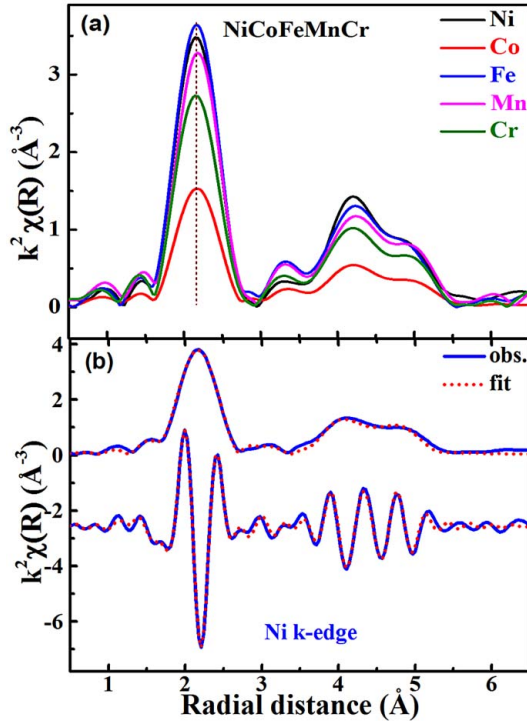
and the corresponding atomic displacement is  $\sim 0.035 \text{\AA}$ . The lattice parameter and Debye factors of NiCoFeMnCr measured with XRD, PDF and ND are listed in Table 1. In fact, the lattice constant of NiCoFeMnCr has nearly no changes below 50 K, and the Debye factor at 50 K is the upper limit of the intrinsic lattice distortion, which corresponds to an atomic displacement value of  $\sim 0.41 \text{\AA}$ . From XRD and ND measurements, the average atomic displacement in NiCoFeMnCr HEA at zero K due to size mismatch is thus between 0.035 and 0.041  $\text{\AA}$ .

In order to identify the local structure of individual atoms in HEAs, EXAFS measurements were conducted at the  $k$ -edge of each element for NiCoFeMnCr HEA. The FT of EXAFS was derived with Athena program and the fitting of FTs was performed using Artemis software. By keeping the same  $k$ -range ( $3\text{--}11 \text{\AA}^{-1}$ ), the  $k^2$ -weighted FTs of NiCoFeMnCr solid solution alloy at the  $K$ -edge of each element is shown in Figure 3(a). The similar characters of the FTs suggest a very close bonding environment of different atoms in the solid solution alloy. However, the first peak of each element is not exactly in the same  $r$  space, especially to Mn atom, which shifts to



**Table 1.** Lattice parameter  $a$  and isotropic thermal factors (or Debye factors) of NiCoFeMnCr single phase solid solution alloy measured with different methods ( $B_{\text{iso}} = 8\pi^2 U_{\text{iso}}$ ,  $U_{\text{iso}} = \langle \sigma^2 \rangle$ ).

Method	XRD	X-ray PDF	ND	EXAFS
$a$ (Å)	3.5993(1)	3.5825(4)	3.5942 (1)	3.58(1)
Debye factor (Å <sup>2</sup> )	$B_{\text{iso}} = 0.37(3)$	$U_{\text{iso}} = 0.0050$ (9) ( $B_{\text{iso}} = 0.39$ )	$B_{\text{iso}} = 0.393(9)$ (300 K) $B_{\text{iso}} = 0.151(6)$ (50 K)	$\sigma^2 = 0.007(1)$

**Figure 3.**  $k^2$ -weighted FTs of EXAFS function of NiCoFeMnCr solid solution alloy at the  $k$ -edge of individual elements; (b) The fit of Ni  $k$ -edge FT EXAFS function with the random fcc structure model.  $k$ -range:  $3.0\text{--}11\text{Å}^{-1}$ ,  $r = 1.5\text{--}5\text{Å}$  is fitted.

a little larger  $r$ -value. In order to fit the FTs and obtain the local bonding information, a randomly distributed cluster model (fcc) with 55 atoms in a diameter of less than  $5.2\text{Å}$  is built. Single and multi-scattering paths from atoms in the first 4 shells around the core atom are taken into account. There will be too many parameters to fit because of 5 different elements in the alloy. Since all the five elements in the solid solution alloy have similar size, similar bonding environment and similar X-ray scattering cross section, it is difficult to distinguish them with X-ray. In order to make the refinement possible, we use a simple model, which smears the difference of each element in the same shell. The core atom is assumed to have the same bond distances with neighboring atoms of different species in the same shells and the corresponding D-W factors are also assumed to be the same. Besides the magnitude,  $E_0$  and bond length correction parameters, four D-W factors are refined for the atomic pairs between the core atoms and the atoms in the first 4 nearest neighbors. The  $k$ -range is  $3\text{--}11\text{Å}^{-1}$  for all the FTs

**Table 2.** The distance of the nearest atomic pairs in NiCoFeMnCr and the D-W factors derived from the fitting of FTs of EXAFS.

Core atom	$R$ (Å)	$\sigma^2$ : (Å <sup>2</sup> )
Ni	2.53 (1)	0.007 (2)
Co	2.53 (1)	0.007 (1)
Fe	2.53 (1)	0.007 (1)
Mn	2.54 (1)	0.006 (1)
Cr	2.53 (1)	0.007 (1)

and peaks in the region of  $1.5\text{--}5\text{Å}$  radial distance are fitted. Figure 3(b) shows the fitting results of Ni  $K$ -edge FTs, where the fitting is pretty good in radial distance of less than  $5\text{Å}$ . The nearest neighbor atomic pair distances and the corresponding Debye–Waller factors from the fitting are listed in Table 2. The nearest atomic pair distance is  $2.53(1)\text{Å}$  for Ni, Co, Fe and Cr as the core atom. Mn atoms have a little larger distance with its nearest neighbors ( $2.54(1)\text{Å}$ ), which is consistent with the FTs shown in Figure 3(a). The average Debye–Waller factor for all the pairs is around  $0.007\text{Å}^2$ . From ND measurements, the isotropic thermal factors of NiCoFeMnCr at 300 K is  $B_{\text{iso}} = 0.393(9)\text{Å}^2$ , and the corresponding D-W factor is  $\sigma^2 = 0.005\text{Å}^2$ . The D-W factor obtained from EXAFS analysis is slightly larger than that obtained from the diffraction measurements. This is reasonable because EXAFS only counts the scattering contribution from limited neighbor atoms (first 4 shells in our analysis), while diffraction measures the scattering from long distance periodic atoms. A short-range chemical disorder may exist in HEAs. Since NiCoFeMnCr contains five elements with similar X-ray scattering abilities, it is difficult to characterize the short-range order in this solid solution alloy with X-ray and neutron techniques.

In summary, the structure and Debye factors of NiCoFeMnCr solid solution alloy is quantitatively characterized by X-ray diffraction, X-ray total scattering, time-of-flight ND and EXAFS methods. Chemical complexity induced lattice distortion is identified by the intrinsic vibration at 0 K by extrapolating of the Debye factors from the low temperature ND measurements, and the static atomic displacement is  $0.035\text{--}0.041\text{Å}$ . The EXAFS analysis reveals that Mn atoms in the HEA have a little larger ( $\sim 0.4\%$ ) bond distance with neighboring atoms than those of other elements. The intrinsic lattice distortion in NiCoFeMnCr HEA may play a critical role for the advanced mechanical properties.

## Acknowledgment

This work was supported as part of the Energy Dissipation to Defect Evolution (EDDE), an Energy Frontier Research Center funded by the U.S. Department of Energy, Office of Science, Basic Energy of Sciences. Neutron diffraction measurements used resources at the Spallation Neutron Source, a DOE Office of Science User Facility operated by the Oak Ridge National Laboratory. The X-ray diffraction and total scattering measurement were conducted at the Cornell High Energy Synchrotron Source (CHESS) which is supported by the National Science Foundation and the National Institutes of Health/National Institute of General Medical Sciences under NSF award DMR-1332208. The EXAFS measurement was performed at GeoSoilEnviroCARS (The University of Chicago, Sector 13), Advanced Photon Source (APS), Argonne National Laboratory. GeoSoilEnviroCARS is supported by the National Science Foundation - Earth Sciences (EAR - 1634415) and Department of Energy- GeoSciences (DE-FG02-94ER14466). This research used resources of the Advanced Photon Source, a U.S. Department of Energy (DOE) Office of Science User Facility operated for the DOE Office of Science by Argonne National Laboratory under Contract No. DE-AC02-06CH11357.

## Disclosure statement

No potential conflict of interest was reported by the authors.

## Funding

This work was supported as part of the Energy Dissipation to Defect Evolution (EDDE), an Energy Frontier Research Center funded by the U.S. Department of Energy, Office of Science, Basic Energy of Sciences. Neutron diffraction measurements used resources at the Spallation Neutron Source, a DOE Office of Science User Facility operated by the Oak Ridge National Laboratory. The X-ray diffraction and total scattering measurement were conducted at the Cornell High Energy Synchrotron Source (CHESS) which is supported by the National Science Foundation and the National Institutes of Health/National Institute of General Medical Sciences under NSF award DMR-1332208. The EXAFS measurement was performed at GeoSoilEnviroCARS (The University of Chicago, Sector 13), Advanced Photon Source (APS), Argonne National Laboratory. GeoSoilEnviroCARS is supported by the National Science Foundation - Earth Sciences (EAR - 1634415) and Department of Energy- GeoSciences (DE-FG02-94ER14466). This research used resources of the Advanced Photon Source, a U.S. Department of Energy (DOE) Office of Science User Facility operated for the DOE Office of Science by Argonne National Laboratory under Contract No. DE-AC02-06CH11357.

## ORCID

Fuxiang Zhang  <http://orcid.org/0000-0003-1298-9795>

Yang Tong  <http://orcid.org/0000-0002-4886-9982>

Hongbin Bei  <http://orcid.org/0000-0003-0283-7990>

William J. Weber  <http://orcid.org/0000-0002-9017-7365>

Yanwen Zhang  <http://orcid.org/0000-0003-1833-3885>

## References

- [1] Yeh JW, Chen SK, Lin SJ, et al. Nanostructured high-entropy alloys with multiple principal elements: novel alloy design concepts and outcomes. *Adv Eng Mater.* 2004;6:299–303.
- [2] Cantor B, Chang ITH, Knight P, et al. Microstructural development in equiatomic multicomponent alloys. *Mater Sci Eng A.* 2004;375-377:213–218.
- [3] Miracle DB, Senkov ON. A critical review of high entropy alloys and related concepts. *Acta Mater.* 2017;122: 448–511.
- [4] Zhang Y, Zuo T, Tang Z, et al. Microstructures and properties of high-entropy alloys. *Prog Mater Sci.* 2014;61:1–93.
- [5] Gild J, Zhang Y, Harrington T, et al. High-entropy metal diborides: a new class of high-entropy materials and a new type of ultrahigh temperature ceramics. *Sci Rep.* 2016;6:37946.
- [6] Zhang Z, Mao MM, Wang J, et al. Nanoscale origins of the damage tolerance of the high-entropy alloy CrMnFe-CoNi. *Nat Comms.* 2015;6:10143.
- [7] Li Z, Pradeep KG, Deng Y, et al. Metastable high-entropy dual-phase alloys overcome the strength-ductility trade-off. *Nature.* 2016;534:227–230.
- [8] Chuang MH, Tsai MH, Wang WR, et al. Microstructure and wear behavior of  $\text{Al}_x\text{Co}_{1.5}\text{CrFeNi}_{1.5}\text{Ti}_y$  high-entropy alloys. *Acta Mater.* 2011;59:6308–6317.
- [9] Tang Z, Huang L, He W, et al. Alloying and processing effects on the aqueous corrosion behavior of high-entropy alloys. *Entropy.* 2014;16:895–911.
- [10] Zhang Y, Stocks GM, Jin K, et al. Influence of chemical disorder on energy dissipation and defect evolution in concentrated solid solution alloys. *Nat Comms.* 2015;6:8736.
- [11] Yeh JW. Recent progress in high-entropy alloys. *Ann Chim Sci Mat.* 2006;31:633–648.
- [12] Jin K, Sales BC, Stocks GM, et al. Tailoring the physical properties of Ni-based single-phase equiatomic alloys by modifying the chemical complexity. *Sci Rep.* 2016;6:20159.
- [13] Otto F, Dlouhy A, Pradeep KG, et al. Decomposition of the single-phase high-entropy alloy CrMnFeCoNi after prolonged anneals at intermediate temperatures. *Acta Mater.* 2016;112:40–52.
- [14] Lu C, Yang T, Jin K, et al. Radiation-induced segregation on defect clusters in single-phase concentrated solid-solution alloys. *Acta Mater.* 2017;127:98–107.
- [15] He MR, Wang S, Shi S, et al. Mechanisms of radiation-induced segregation in CrFeCoNi-based single-phase concentrated solid solution alloys. *Acta Mater.* 2017;126: 182–193.
- [16] Santodonato LJ, Zhang Y, Feyngenson M, et al. Deviation from high-entropy configurations in the atomic distributions of a multi-principal-element alloy. *Nat Comms.* 2015;6:5964.
- [17] Diao H, Santodonato LJ, Tang Z, et al. Local structures of high-entropy alloys (HEAs) on atomic scales: an overview. *JOM.* 2015;67:2321–2325.
- [18] Song H, Tian F, Hu QM, et al. Local lattice distortion in high-entropy alloys. *Phys Rev Mater.* 2017;1:023404.
- [19] Toda-Caraballo I, Rivera-Diaz-del-Castillo PEJ. A criterion for the formation of high entropy alloys based on lattice distortion. *Intermetallics.* 2016;71:76–87.

- [20] Owen LR, Pickering EJ, Playford HY, et al. An assessment of the lattice strain in the CrMnFeCoNi high-entropy alloy. *Acta Mater.* **2017**;122:11–18.
- [21] Gludovatz B, Hohenwarter A, Catoor D, et al. A fracture-resistant high-entropy alloy for cryogenic applications. *Science.* **2014**;345:1153–1158.
- [22] Varvenne C, Luque A, Curtin WA. Theory of strengthening in fcc high entropy alloys. *Acta Mater.* **2016**;118:164–176.
- [23] Tong Y, Jin K, Bei H, et al. Quantitative analysis of local lattice distortion in medium and high-entropy alloys. Submitted. 2017.
- [24] Tulip PR, Staunton JB, Lowitzer S, et al. Theory of electronic transport in random alloys with short-range order: Korringa-Kohn-Rostoker nonlocal coherent potential approximation. *Phys Rev B.* **2008**;77:165116.
- [25] Zhang FX, Zhao S, Jin K, et al. Local structure and short-range order in a NiCoCr solid solution alloy. *Phys Rev Lett.* **2017**;118:205501.
- [26] Linden Y, Pinkas M, Muntiz A, et al. Long-period antiphase domains and short-range order in a B2 matrix of the AlCoCrFeNi high-entropy alloy. *Scr Mater.* **2017**;139:49–52.
- [27] Schneeweiss O, Friak M, Dudova M, et al. Magnetic properties of the CrMnFeCoNi high-entropy alloy. *Phys Rev B.* **2017**;96:014437.
- [28] Hammersley AP. Fit 2d, ESRF, Grenoble, France, 1998.
- [29] Rodriguez-Carvajal J. Recent developments of the program FULLPROF, in commission on powder diffraction (IUCr). *Newsletter.* **2016**;26:12–19.
- [30] Ravel B, Newville M. ATHENA, ARTEMIS, HELPAES-TUS: data analysis for X-ray absorption spectroscopy using IFEFFIT. *J Synch Rad.* **2005**;12:537–541.
- [31] Peng LM, Ren G, Dudarev SL, et al. Debye–waller factors and absorptive scattering factors of elemental crystals. *Acta Cryst A.* **1996**;52:456–470.